

Algorithms and Architectures for X-Ray Diffraction Tomography

Ke Chen and David Castañón
{ck, [dac](mailto:dac@bu.edu)}@bu.edu

This work was sponsored by DHS S&T under the ALERT
Center of Excellence



Electrical & Computer Engineering

Summary

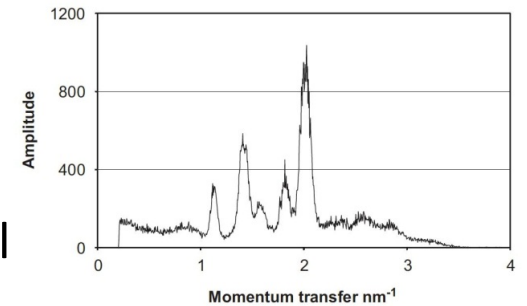


- Iterative reconstruction algorithms for reconstruction of XDI images
 - Good localization, characterization of materials with strong Bragg peaks
 - Harder: accurate reconstruction of liquids and other amorphous materials in the presence of stronger scatterers nearby
- XDI architectures with coded apertures and limited illumination directions leads to good reconstruction of volumetric and spectral images
 - increased scatter signal strength, better conditioned reconstruction
- Iterative reconstruction algorithms are essential in these architectures
 - Needed to mitigate artifacts from “strong” scatterers, obtain observability exploiting sparsity and spatial consistency
- Need fusion with CT or equivalent normalization for reconstruction
- Major challenges remain:
 - Computation requirements for reconstruction
 - Architecture design for improved signal/noise ratio
 - Explosives detection/classification using reconstructed signals for liquids and HME classes

Motivation

Background:

- ❑ Material identification based on conventional X-ray computed tomography (CT) images can be **ambiguous**
- ❑ **X-ray diffraction imaging (XDI)** systems identify material based on coherent-scatter form factor – New signature that depends on molecular structure



Coherent-scatter form factor of TNT
(Harding '09, Morpho)

Issues:

- ❑ Weak signals may require long collection times
- ❑ What are appropriate algorithms and architectures?

Existing XDI Commercial Product:

- ❑ Single view, direct imaging

Focus of Talk: Discuss recent progress and results on algorithms for different XDI architectures



Morpho XRD 3500™

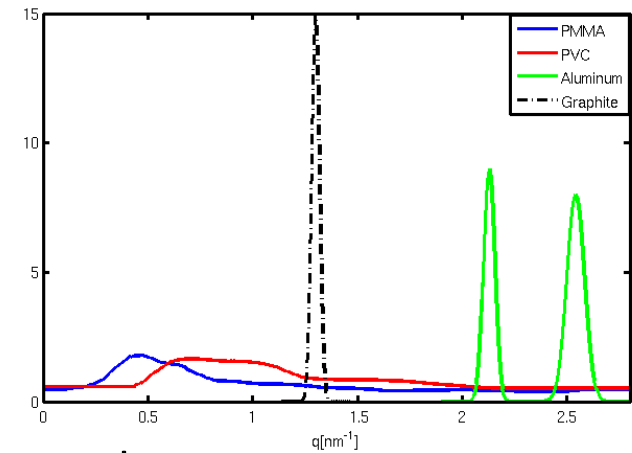
X-ray Diffraction Imaging

- Construct the *coherent-scatter form factor* $|F(q,\mathbf{x})|^2$ at all positions \mathbf{x} in volume of interest: **4-dimensional function!**
 - Expressed as distribution of **transferred momentum** q that causes the deviation of photon of wavelength λ by angle θ

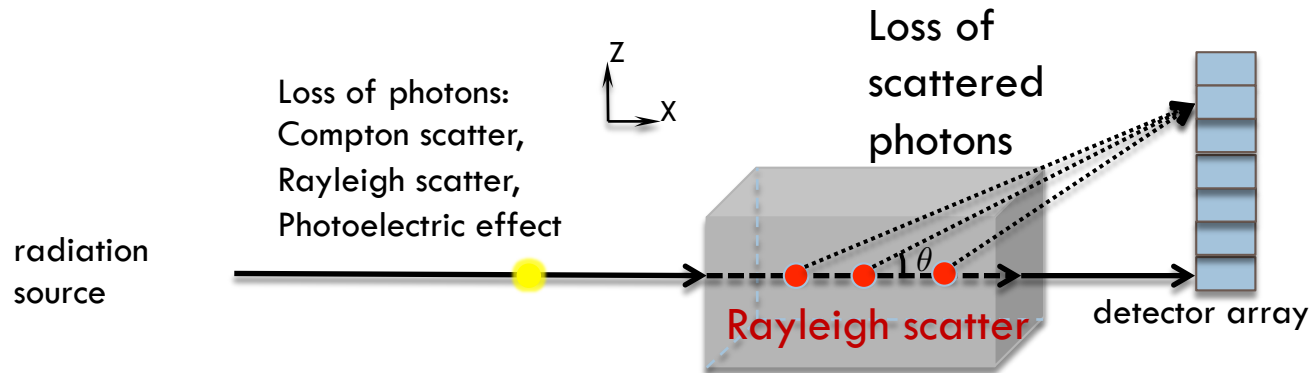
$$q = \frac{1}{\lambda} \sin\left(\frac{\theta}{2}\right)$$

Form factors

- For crystalline materials, **Bragg peaks** reveal molecular composition for material discrimination in terms of preferred scattering angles
- For amorphous materials, or liquids, form factor is smoother



X-ray Diffraction Principles



Observations:

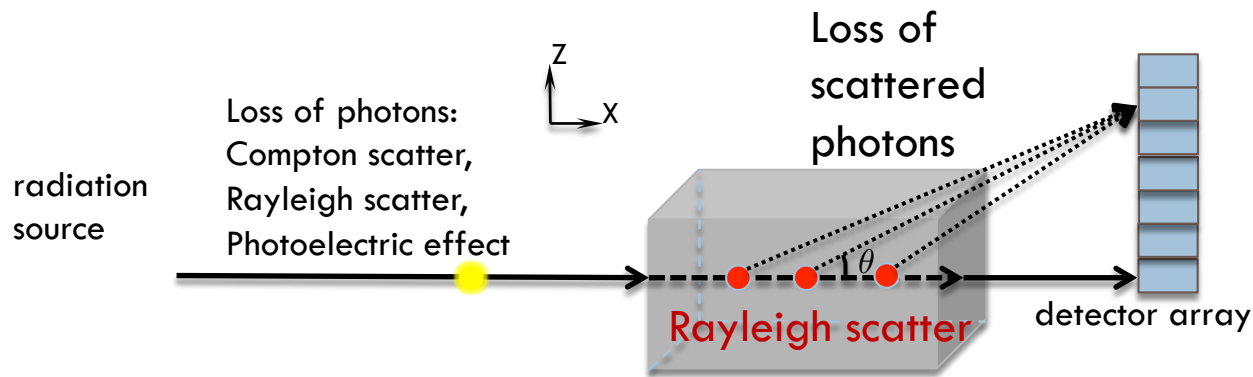
- ❑ Fraction of photons that are scattered coherently is small – fraction decreases with increasing photon energy
- ❑ Fraction of photons that are lost to photoelectric effect also decreases with increasing photon energy

- ➔ Low energy Rayleigh scatter will be highly attenuated
- ➔ High energy Rayleigh scatter is less likely



Weak signals!
Limit on effective energy band

X-ray Diffraction Principles - 2



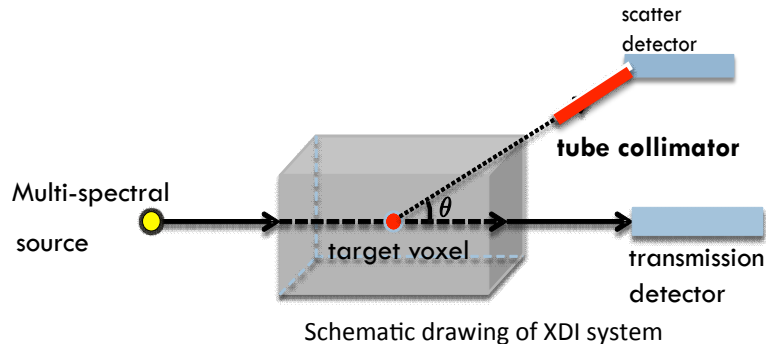
Observations 2:

- ❑ Depending on collimation scheme and source spectrum, each detector measures scatter from different locations and different energies
- ❑ Detector technology: photon counting detectors vs intensity detectors
 - ❑ Slice reconstruction: 3-D object may be easier to reconstruct from 2-D array of photon counting detectors, equivalent to 3-D measurement
 - ❑ Alternative: few views with intensity measurements (not many, though...): compressive sensing reconstruction

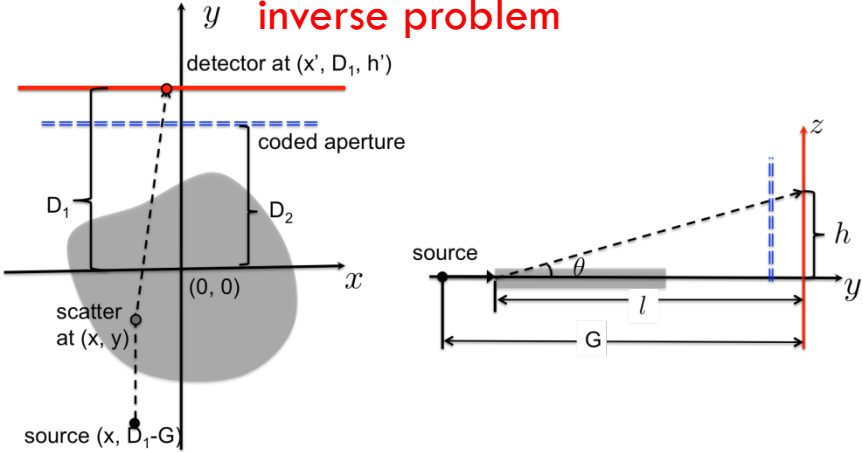
X-Ray Diffraction: Some Architectures



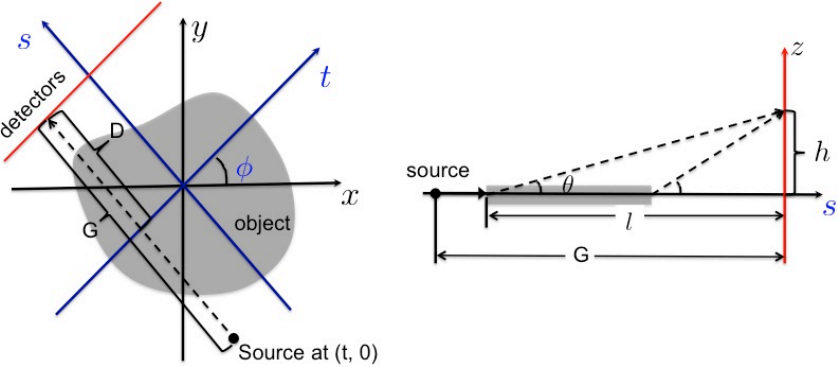
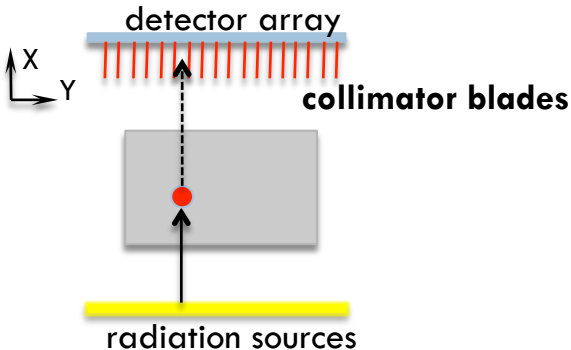
Direct imaging: tube collimators
Photon-inefficient but simple algorithms



Coded aperture imaging:
Captures more photons, complex inverse problem



Limited-angle tomography: sheet collimators
Higher SNR, often requires rotating detectors and tomography algorithms



Model depends on architecture :

- Example below for intensity detectors, sheet collimators separating vertical lines of detectors

$$I_\phi(t, h) = \int_0^G \int_{\lambda_m^{in}}^{\lambda_m^{ax}} I_\lambda(t, 0) \mathcal{A}_\lambda(t, 0, s, 0) \mathcal{B}_\lambda(t, s, G, h) \frac{|F(t, s, q)|^2}{[(G - s)^2 + h^2]^{3/2}} d\lambda ds$$

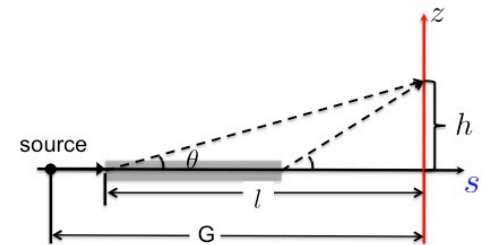
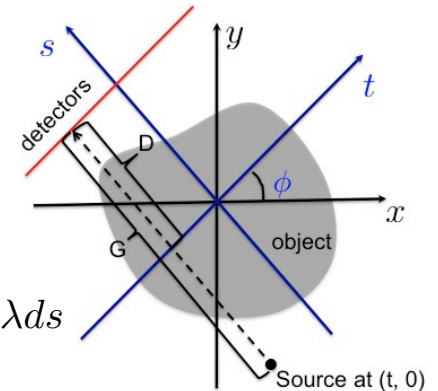
$$q = \frac{\sin(0.5 \tan^{-1}(\frac{h}{G-s}))}{\lambda} \approx \frac{h}{2\lambda(G - s)}$$

$I_\lambda(t, 0)$: incident x-ray intensity at λ ;

$\mathcal{A}_\lambda(t, 0, s, 0)$:attenuation for λ along incoming ray from 0 to s ;

$\mathcal{B}_\lambda(s, 0, G, h)$:attenuation along the scattered ray from $(s, 0)$ to (G, h) .

$|F(t, s, q)|^2$:coherent-scatter form factor at location (t, s)



- For photon counting detectors, model changes:

$$I_\phi(t, h, \lambda_0) = \int_0^G \int_{\lambda_0}^{\lambda_0 + \Delta} I_\lambda(t, 0) \mathcal{A}_\lambda(t, 0, s, 0) \mathcal{B}_\lambda(t, s, G, h) \frac{|F(t, s, q)|^2}{[(G - s)^2 + h^2]^{3/2}} d\lambda ds$$

XDI Math 2

- Easy extensions to include other architectures
 - ▣ Different collimators or coded aperture masks, fan beams, ...
- Important issue: Need to account for attenuation in both the excitation path and the scatter path
- Two approaches possible
 - ▣ Estimate attenuation using dual-energy conventional CT reconstruction and incorporate into image reconstruction process -- general
 - ▣ Normalize path loss using direct path observation
 - Small angle assumption: attenuation along the path of scattered radiation is approximately same as on transmitted path
 - More appropriate for photon-counting detectors (small energy range per measurement)

$$J_{\phi}(t, h) = \frac{I_{\phi}(t, h)}{I_{\phi}(t, 0)} \approx \int_0^G \int_{\lambda_{min}}^{\lambda_{max}} \frac{|F(t, s, q)|^2}{[(G - s)^2 + h^2]^{3/2}} d\lambda ds$$

Iterative Reconstruction

- Algorithm 1 (IRL1):
 - ▣ Iterative reconstruction, slice by slice
 - ▣ Look for spatial coherence in form factor reconstructions among nearby voxels
 - ▣ Sparsity in form factors representation
- Convex optimization formulation
$$\min_{\underline{\mathbf{x}}} (\underline{\mathbf{y}} - C\underline{\mathbf{x}})^T W(\underline{\mathbf{y}}) (\underline{\mathbf{y}} - C\underline{\mathbf{x}}) + \alpha^2 \sum_{m=1}^M \|D\underline{\mathbf{x}}\|_1$$
 - ▣ $\underline{\mathbf{y}}$: measurements, stacked by voxels and momentum transfer
 - ▣ $\underline{\mathbf{x}}$: reconstructed form factors over voxels
 - ▣ C : Discretized observation matrix
 - ▣ D : Spatial derivative operator
 - ▣ M : Number of form factor bins
- Solve using standard convex techniques

Iterative Reconstruction

- Algorithm 2 (IREP):
 - ▣ Iterative reconstruction, slice by slice
 - ▣ Look for spatial coherence in form factor reconstructions among
 - ▣ Simultaneous segmentation/image formation avoiding smoothing across edges (Ambrosio-Tortorelli)

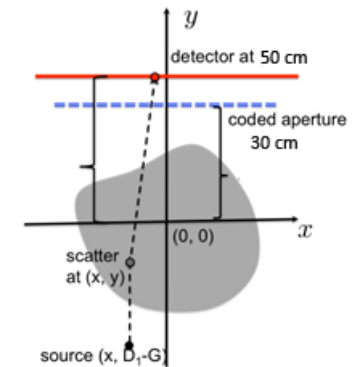
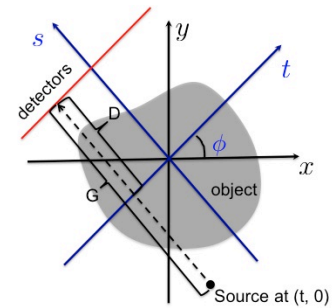
$$\min_{(\mathbf{x}, \mathbf{s})} \|\mathbf{y} - C\mathbf{x}\|_{W(\mathbf{y})}^2 + \alpha_1^2 \sum_{m=1}^M \|\mathbf{D}\mathbf{x}_m\|_{\mathbf{W}_s}^2 + \varphi_s(\mathbf{s}, \gamma)$$

$$W_s = \text{Diag} [(1 - [\mathbf{s}]_i)^2], \quad \varphi_s(\mathbf{s}, \gamma) = \gamma^2 \|\mathcal{D}\mathbf{s}\|^2 + \frac{1}{\gamma^2} \|\mathbf{s}\|^2$$

- Solve using biquadratic iterative optimization
- Other algorithms investigated (overcomplete basis representations, ...) with similar results.

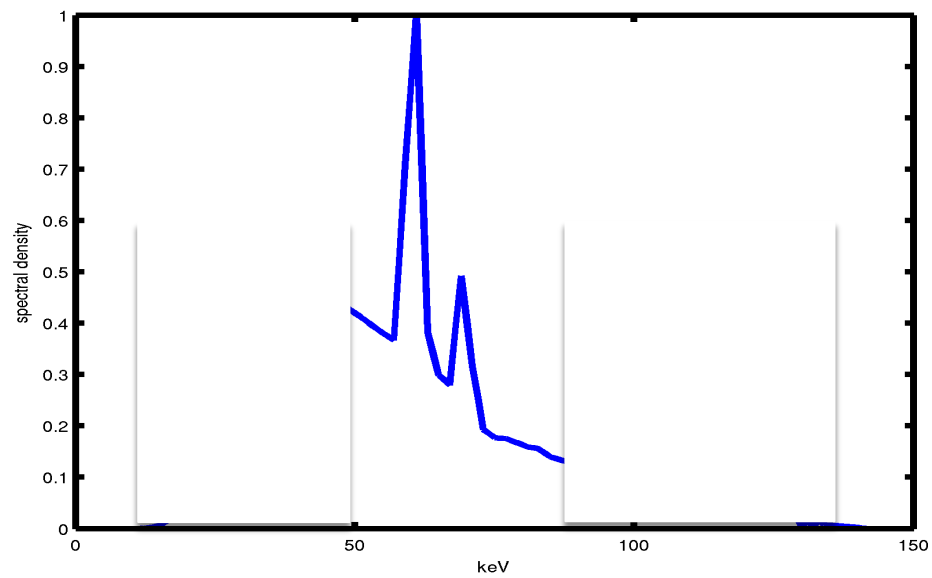
Experiments

- Architecture 1: Limited angle tomography with vertical collimation
 - ▣ 7 views, from -60 to 60 degrees, 20 degrees apart
- Architecture 2: Coded aperture, single view
- Architecture 3: Coded aperture, 3 views (-60,0,60)
 - ▣ Simple coded aperture design (Brady et al '12)
 - ▣ Focus on reconstruction
- Detectors
 - ▣ Intensity detectors
 - ▣ Photon counting detectors, 6 keV resolution
- Issues:
 - ▣ 3-D slice reconstructions from very few 2-D views



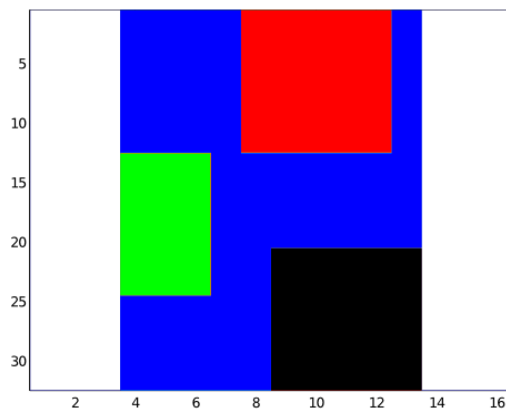
Illumination Variations

- Monochromatic source at 72 keV
- Polychromatic source from 50 keV to 80 keV with basic spectra
- Simulated Monte Carlo photon sources

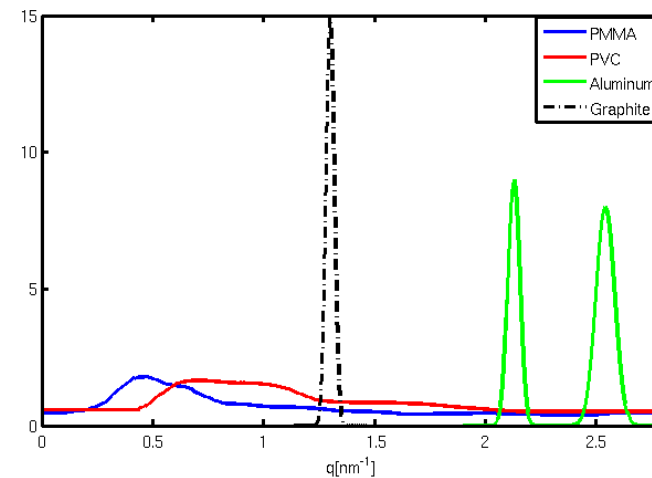


Experiment Phantom

- Object of size 8*4cm, composed of 4 elements (PMMA, PVC, Aluminum, Graphite)
- Two phantoms: a flat plate, 1 cm tall, and a tall rectangular solid, 40 cm tall
- Focus on clutter, interference, attenuation
 - Different attenuation of scatter



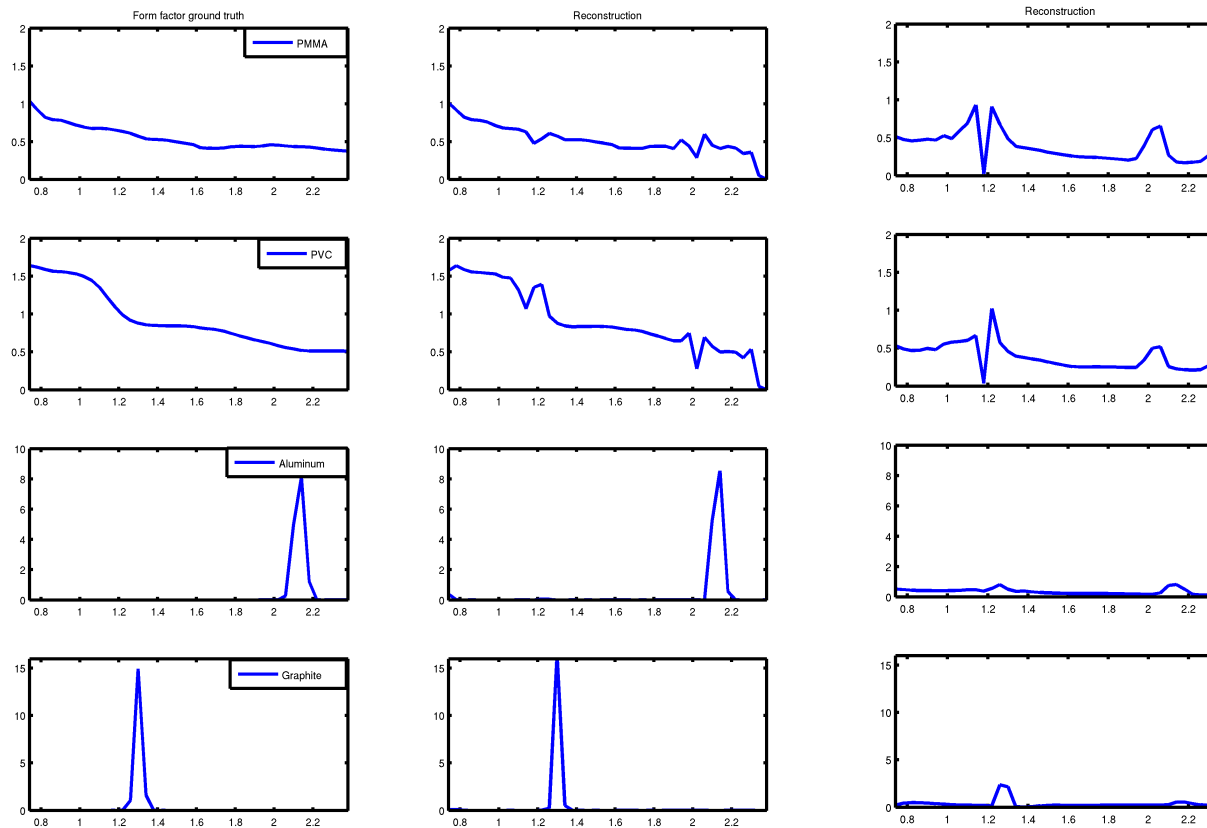
Plan view of object in
Illumination plane



Form factors for the elements

Experiment 1: Why Coded Aperture

- Phantom: Thin plate
- Architecture: **with and without coded aperture**, 3 views (-60, 0, 60) degrees, with **intensity detectors, single energy illumination (72 keV)**, no noise, IRL1 algorithm



Truth

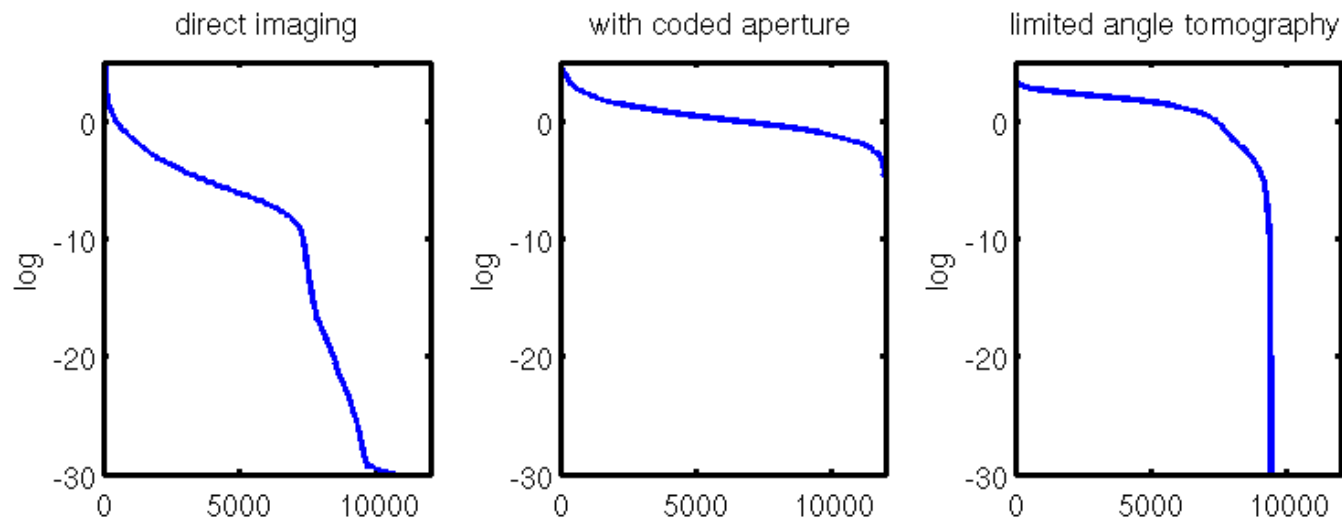
With coded aperture

Without coded aperture

Explanation

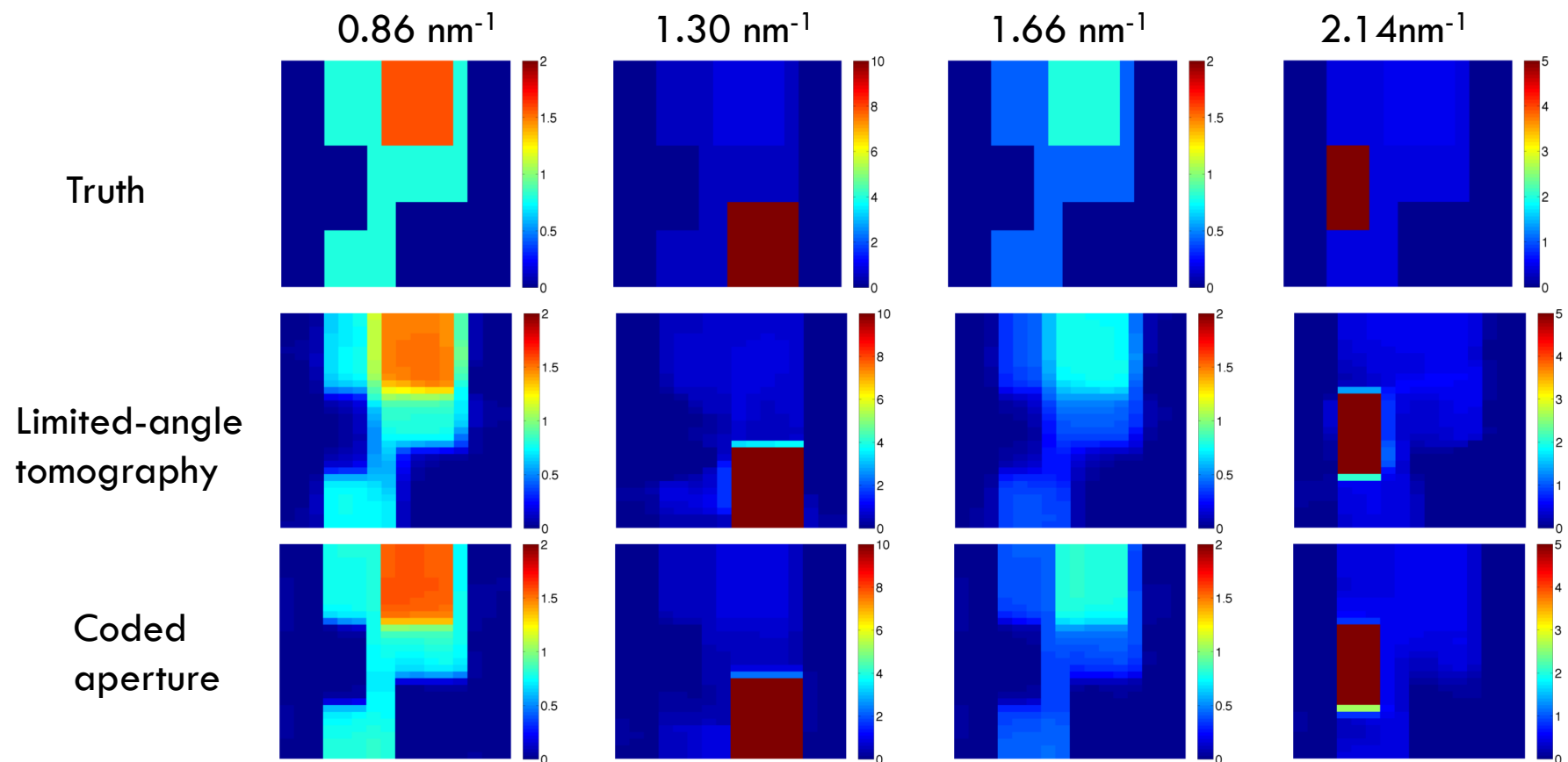
- Without coded aperture, limited angle tomography results in ill conditioned inverse problem
 - ▣ Hard to separate different material contributions

Comparison of log of singular values for different architectures



Experiment 2: Coded aperture vs vertical collimation

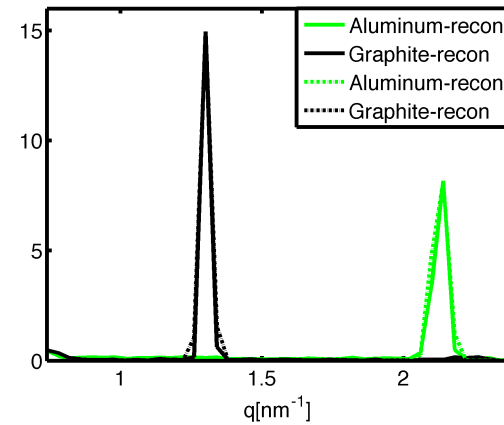
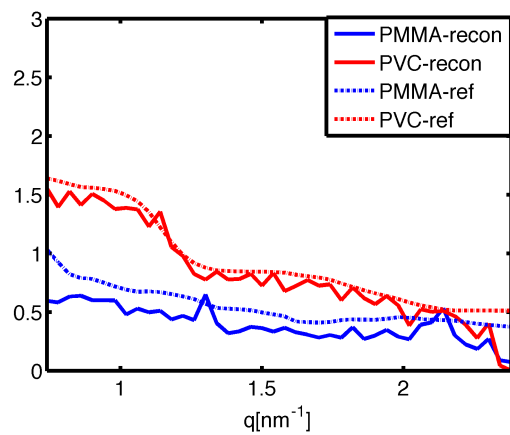
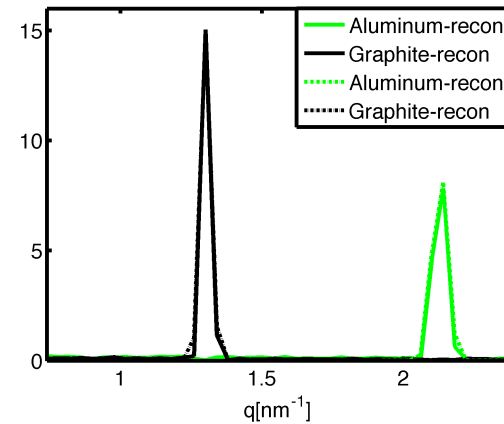
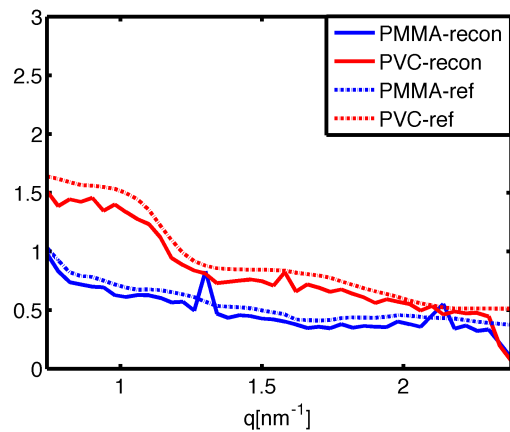
- Phantom: **thin plate**
- Architectures: Coded aperture, 3 views (-60, 0, 60) degrees and limited angle tomography with vertical collimators, 7 views, **intensity detectors**, single-energy at 72 keV, IRL1 algorithm



Main difference: More efficient collection of scattered photons in coded aperture – Increased signal strength

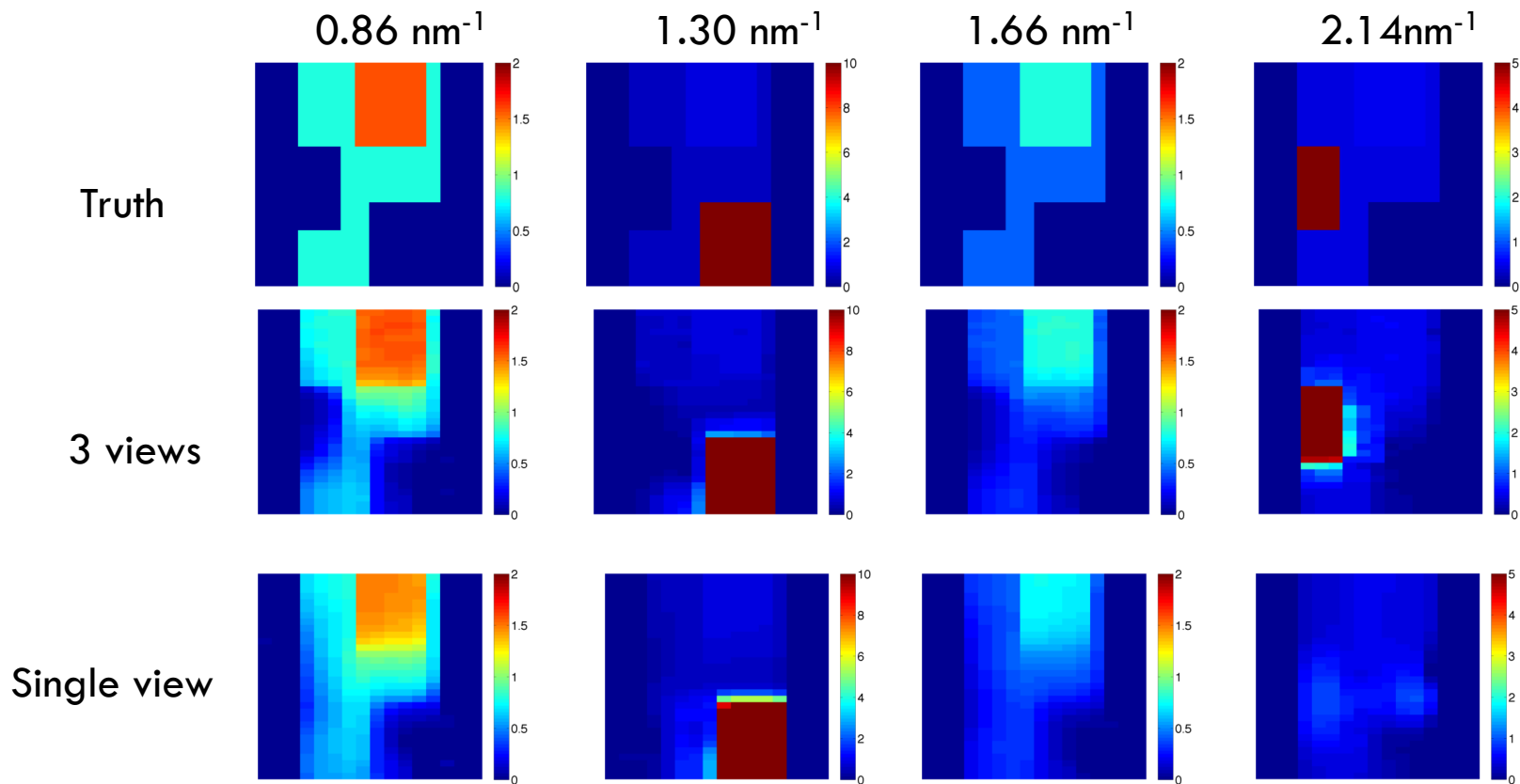
Form Factor Reconstructions

- Average over region of the materials



Experiment 3: Why Multiview?

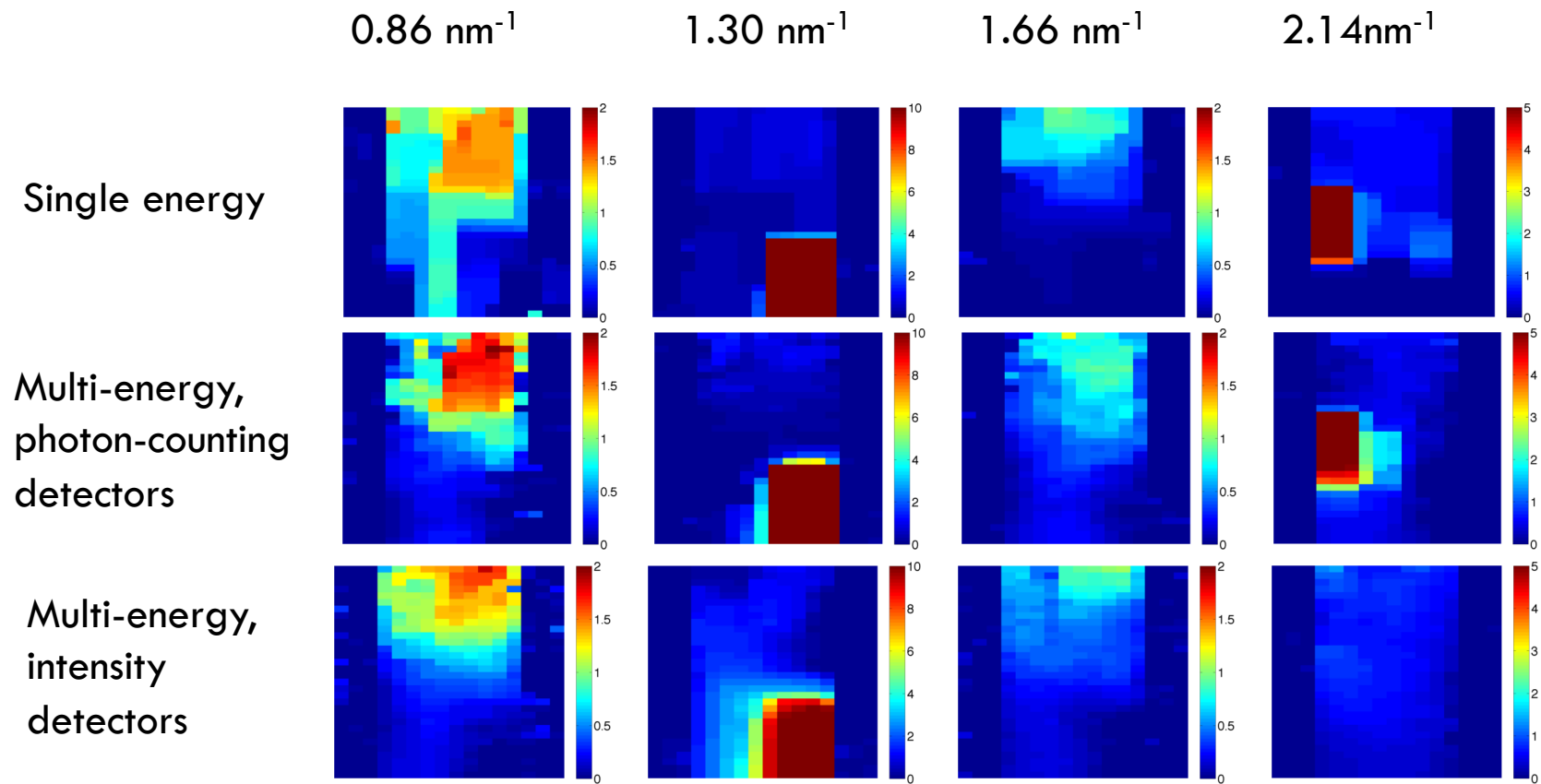
- Phantom: **Tall rectangular solid**
- Architecture: Coded aperture, **3 views** (-60, 0, 60) degrees, vs **single view**, 0 degrees, with **photon-counting detectors**, multi-energy illumination, IRL1



Strong absorption from a single view can reduce scatter signal (no aluminum...)

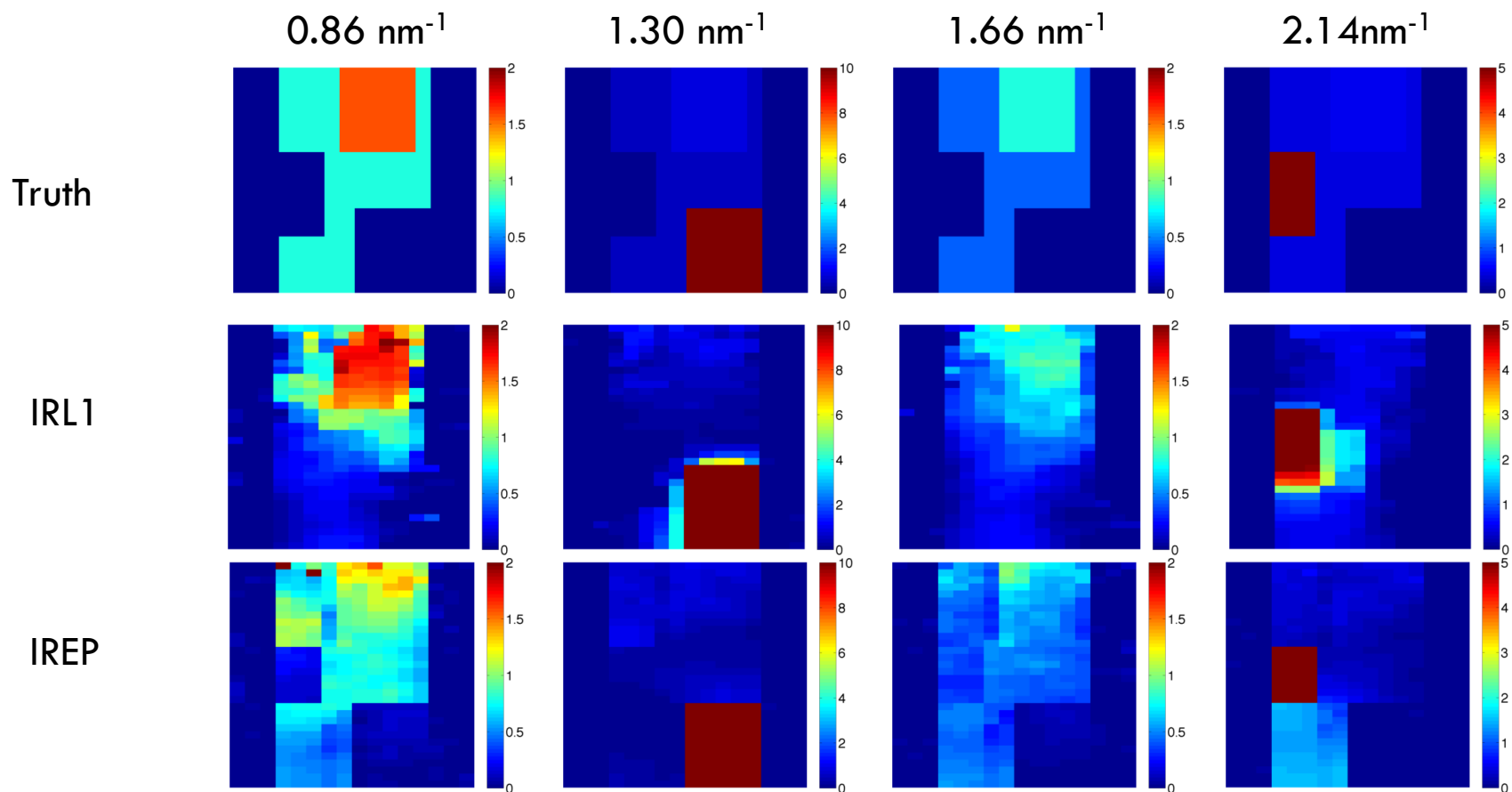
Experiment 4: Photon-counting detectors help

- Phantom: **Tall rectangular solid**
- Architecture: Coded aperture, 3 views (-60, 0, 60) degrees, with **intensity detectors and photon-counting detectors**, **monochromatic vs multi-energy** illumination, IRL1



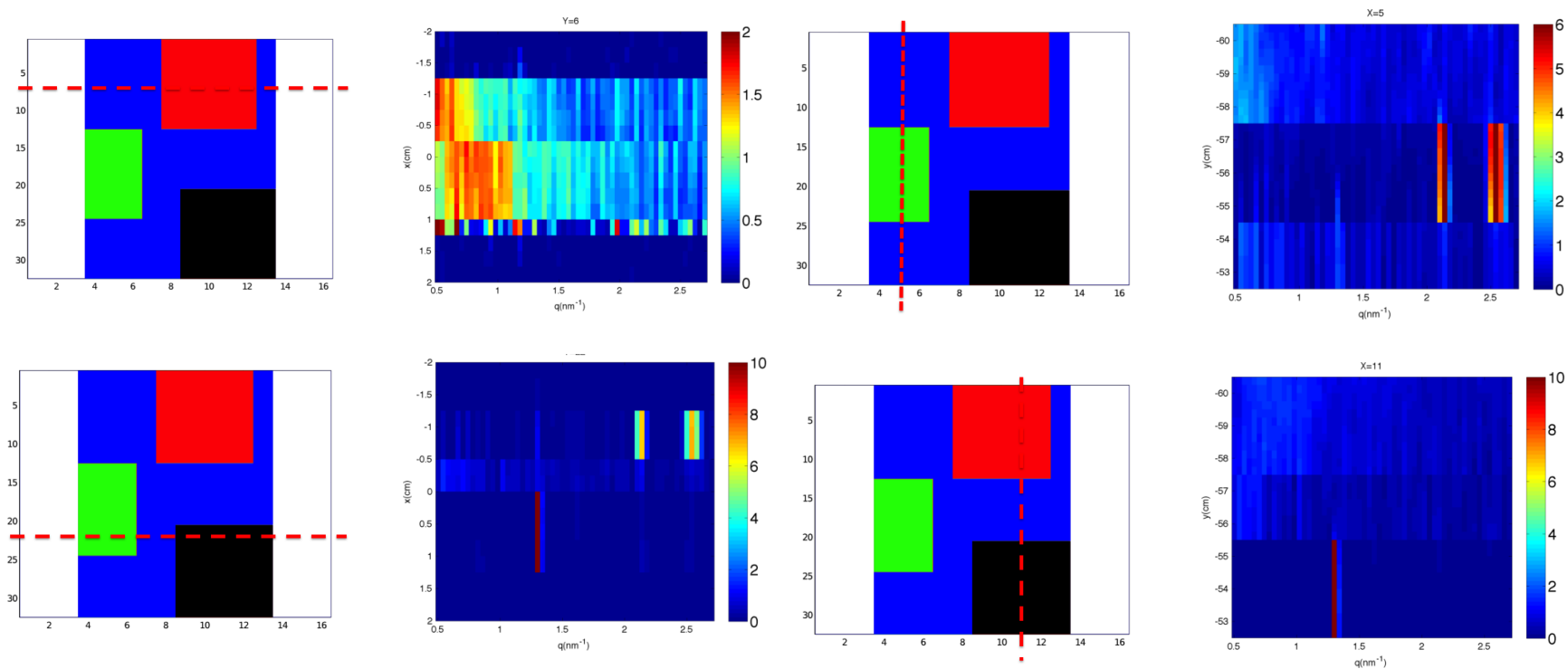
Experiment 5: Algorithm choices

- Phantom: Tall rectangular solid
- Architecture: Coded aperture, 3 views (-60, 0, 60) degrees, with **photon-counting detectors**, multi-energy illumination, IRL1 and IREP algorithms



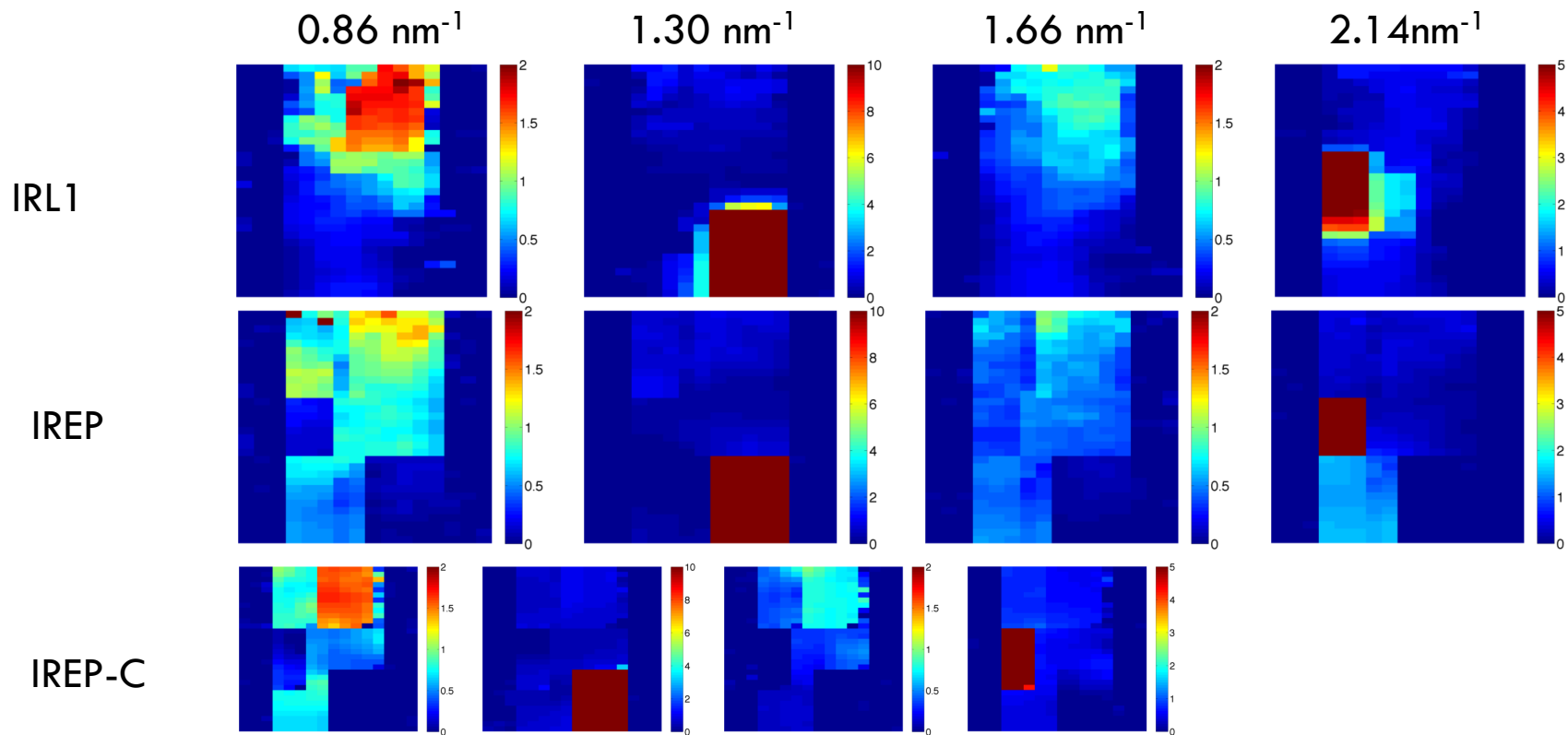
A Different View: Segmentation

- Showing form factors of X, Y slices: Can segment, approximately...



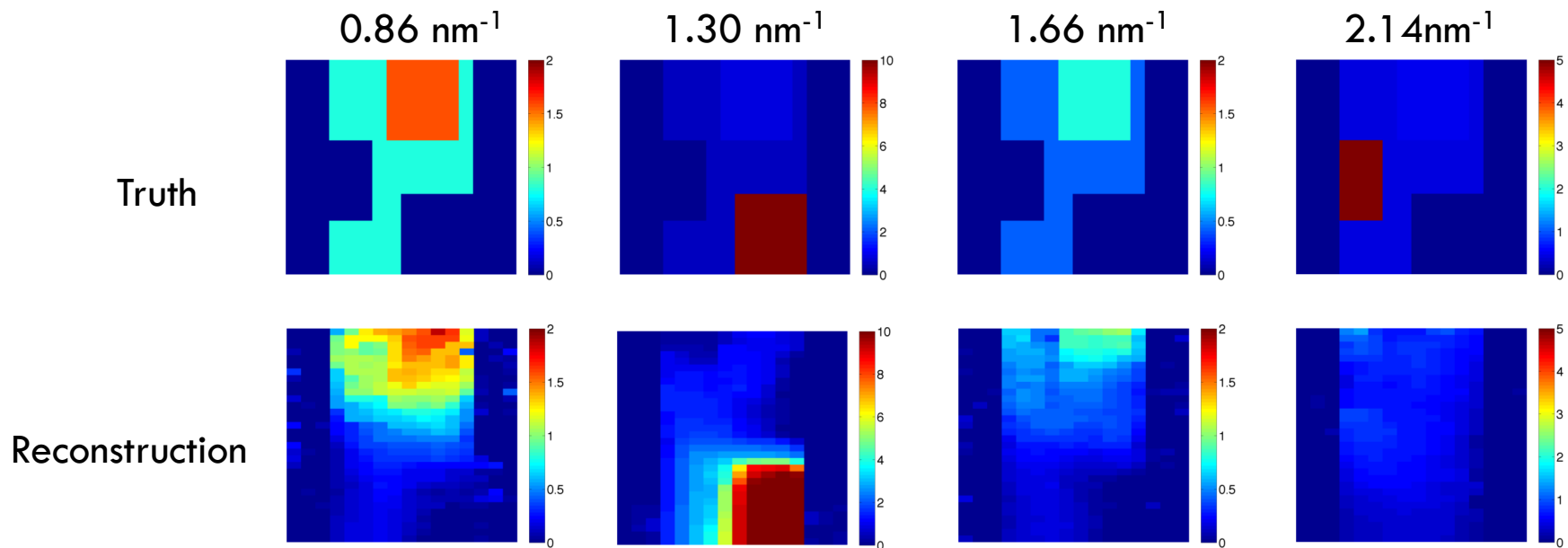
Avoiding Local Minima

- Initialize IREP after Segmentation

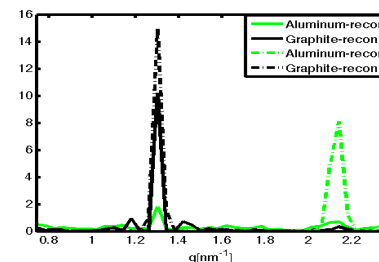
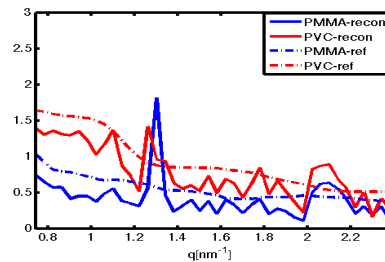


Experiment 6

- Phantom: Tall rectangular solid, reconstructing a slice
- Architecture: Coded aperture, 3 views (-60, 0, 60) degrees, with **intensity detectors**, multi-energy illumination, **ideal noiseless case**



Estimated form factors, averaged over true region



Summary



- Iterative reconstruction algorithms are promising for reconstruction of XDI images
 - ▣ Good localization and characterization of materials with well-defined Bragg peaks
 - ▣ Harder to get accurate reconstruction of liquids and other amorphous materials in the presence of stronger scatterers nearby
- Architectures with photon-counting detectors offer improved reconstruction
 - ▣ Higher dimensional measurement, better conditioned reconstruction
- Attenuation correction requires fusion with CT or equivalent normalization for different architectures
- Major challenges remain:
 - ▣ Computation requirements for reconstruction
 - ▣ Architecture design for improved signal/noise ratio
 - ▣ Explosives detection/classification using reconstructed signals for liquids and HME classes